© Malaysian Journal of Anaesthesiology 2025; 4:139-156
Original article
https://doi.org/10.35119/myja.v4i2.96

Effectiveness of a biological isolation chamber in containing and evacuating aerosolised particles during simulated patient transport

Huzaifah **Abdul Wahab**[1], Murnira **Othman**[2], Muhammad Ikram **A. Wahab**[3], Azarinah **Izaham**[4], Rufinah **Teo**[4], Siti Nidzwani **Mohamad Mahdi**[4]

[1]Department of Anaesthesia and Critical Care, Hospital Kuala Lumpur, Kuala Lumpur, Malaysia; [2]Institute for Environment and Development (LESTARI), Universiti Kebangsaan Malaysia, Selangor, Malaysia; [3]Centre for Toxicology and Health Risk Studies, Faculty of Health Science, Universiti Kebangsaan Malaysia, Selangor, Malaysia; [4]Department of Anaesthesiology and Intensive Care, Hospital Canselor Tuanku Muhriz, Faculty of Medicine, Universiti Kebangsaan Malaysia, Kuala Lumpur, Malaysia

Abstract

Introduction: The BIOBASE biological isolation chamber (BBIC) was used to limit the spread of SARS-CoV-2 transmission during transport of COVID-19 patients. We aim to study the effectiveness of BBIC in limiting the spread of aerosol during static transport amongst healthcare workers.

Methods: Nebulised saline 0.9% was generated to saturate aerosolised particles within the BBIC placed within a constructed outer enclosure. Negative pressure was activated and particulate matter (PM), PM_{10} and $PM_{2.5}$ concentrations were measured over 60 minutes using AS-LUNG sensors placed inside (C_{in}) and outside (C_{out}) the BBIC. Control, closed ports, and open port models were developed to assess the effectiveness of the BBIC in containing and evacuating aerosolised particles. The ratio of measured C_{in} to the measured $C_{out,}$ designated as F_{iso}, ($F_{iso} = C_{in}/ C_{out}$) was derived.

Correspondence: Siti Nidzwani Mohamad Mahdi, Department of Anaesthesiology and Intensive Care, Hospital Canselor Tuanku Muhriz, Faculty of Medicine, Universiti Kebangsaan Malaysia, Jalan Yaacob Latif, Bandar Tun Razak, 56000 Cheras, Kuala Lumpur, Malaysia.
E-mail: nidzwani@hctm.ukm.edu.my

Results: The differences in F_{iso} value of PM_{10} compared to $PM_{2.5}$ in the closed ports test were significant at minute 15 and 25 ($p < 0.001$ respectively). The differences in F_{iso} value of PM_{10} compared to $PM_{2.5}$ in the open ports test was significant at minute 15 ($p < 0.001$), which suggests that both the closed and open ports tests effectively contained the PM_{10} as compared to $PM_{2.5}$ aerosolised particles. The F_{iso} negatively correlated with time for the open ports ($r = -0.79$, $p = 0.035$) and closed ports tests ($r = -0.79$, $p = 0.035$) for PM_{10}.

Conclusions: The closed and open BBIC ports effectively contain and evacuate PM_{10} aerosolised particles during simulation of static transport of COVID-19 patients. The BBIC contains and evacuates PM_{10} more effectively than $PM_{2.5}$ aerosolised particles.

Keywords: aerosolised particles, COVID-19, infectious disease transmission, transportation of patients

Introduction

Severe Acute Respiratory Syndrome Coronavirus 2 (SARS-CoV-2) virus was identified in the respiratory tract of patients with pneumonia in Wuhan, Hubei China in December 2019. The World Health Organization declared the infection a pandemic on March 11 2020.[1] Many measures have been taken to limit spread of SARS-CoV-2 infection. The emergence of more virulent strains of SARS-CoV-2 potentially increases the risk of transmission amongst the public and the healthcare workers.[2-5]

The SARS-CoV2 virus has the capacity to transmit from one host to another via direct or indirect droplet contact or inhalation of suspended nuclei droplets within the atmosphere.[6-10] These droplets are generated from the respiratory tract and have variable particle sizes ranging from 0.25 to 42 µm, depending on the respiratory activity (coughing, sneezing, talking, singing, etc).[11-13] Coughing, heavy breathing, and sneezing generate large amounts of aerosolised particles ranging from 0.35–10 µm.[14-17]

Direct droplet spread refers to droplets generated from the respiratory tract that land on another host's mucosal surface. Indirect droplet spread is when there is a direct physical interaction with the infected host or surfaces in which the infected host has come into contact.[18-19] Airborne transmission occurs when there is inhalation of droplet nuclei or aerosolised particles into the lower airway. The term nuclei droplets are smaller sized droplets, 5 to 10 µm, that may remain

airborne for longer periods of time (from minutes to hours).[20-22] The distance a particle can travel is rather complex and dependent upon many factors including particle size, flow velocity, density, air turbulence, humidity, and particle composition and humidity.[19-24]

Several measures to limit droplet spread in preventing SARS-CoV-2 transmission have been applied. Physical barrier models, including personal protective equipment recommendations, plastic draping segments within intensive care units, barrier chambers, and transport isolation pods (isopods), have been utilized.[25-27] Isopods are physical barrier chamber class I medical devices designed to limit the transmission of highly infectious disease during transport of infected patients.[28-34] The BIOBASE biological isolation chamber (BBIC; BIOBASE model BFG VI; Shandong, China) was used in many major hospitals in Malaysia during the COVID-19 pandemic.[35] However, there are issues with barrier chambers: increased intubation time, longer exposure risk, secondary aerosolization, increased duration of patient transport, disinfection issues, and high cost are among many problems reported.[28-34]

To date, the quantitative data on the effectiveness of the transport barrier chambers to limit aerosol spread during transport of COVID-19 patients is still limited. We aim to study the effectiveness of BBIC in limiting spread of aerosol during simulation of static transport of COVID-19 patient amongst healthcare workers.

Materials and methods

This simulation study was conducted within a 2-week duration in August 2022 following the approval from institutional Secretariat of Research and Innovation as well institutional Research and Ethics Committee.

The BBIC model BFG VI with dimensions of 1900 x 680 x 500 mm and a built-in negative pressure capacity running at a pressure magnitude of 19 Pascals was used in all the simulation tests. There were 3 HEPA filters that filtered particle sizes of 0.3 µm. The chamber was equipped with an all-around zipper system for easy operation. The chamber had 10 integrated glove portals to allow for easy access to the patient and 2 utility portals used for infusions and other medical equipment and were zipped and sealed during transport of COVID-19 patients. Should medical interventions be required, these access ports would be zipped open to conduct necessary procedures (Fig. 1a).

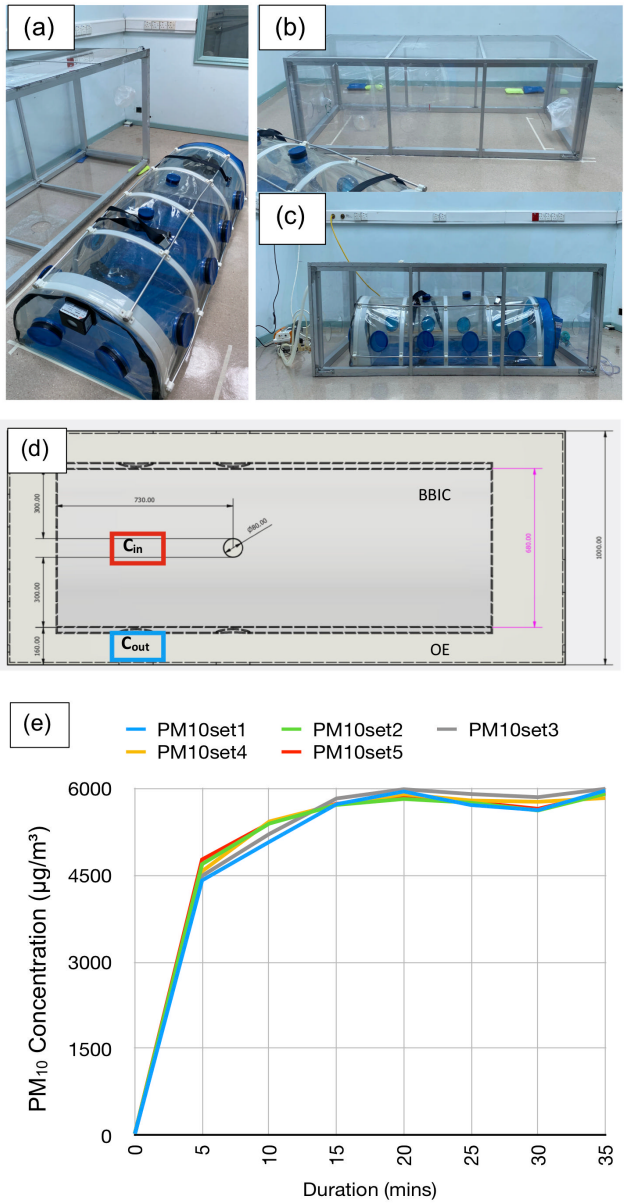

Fig. 1. (a) BBIC. *(b)* Outer enclosure (OE). *(c)* OE encapsulating BBIC. *(d)* Longitudinal view of the OE encapsulating the BBIC. Red square: location of AS-LUNG device measuring C_{in} within BBIC. Blue square: location of AS-LUNG device measuring C_{out}. *(e)* Measured concentration of PM_{10}.

A constructed outer enclosure (OE) was placed encapsulating the BBIC (Fig. 1b and 1c). The OE was to maintain the standard external BBIC environment (room air temperature average 26.2°C, relative humidity average 59.7%, room air pressure of 1 atm), and to provide a standard compartment for generated aerosol particle concentration measurement. The OE was constructed to fix a volume of 2300 x 1000 x 650 mm cuboidal body using polycarbonate material reenforced with an outer-skeletal aluminium structure to contain aerosol particles generated from within and prevent significant air leak to obtain accurate measurement. Several circular access and ventilatory ports were carved out from the polycarbonate body.

A nebulizer with its reservoir filled with 10 cc of normal saline 0.9% was used to deliver nebulized saline 0.9% connected to a flowmeter attached to the wall oxygen source outlet running at a flow rate of 10 l/min, with capacity to generate aerosolised particles with diameter of 3–5 µm. An Electrolux Vacuum Cleaner Fustar 1600-R-140 Model Z1231 was set to run at a suction power of 320 W for purging both the BBIC and OE for a duration of 10 minutes before the start of every experiment set to obtain a standard baseline room air particle concentration.

The particle concentration of the generated aerosols was measured with a device known as the AS-LUNG portable optical particle sensor (Acadamia Sinica, Taipei, Taiwan). A pair of these sensors were used simultaneously, one was placed within the BBIC and the other was placed outside of the BBIC, within the OE compartment (Fig. 1d). This device was able to sense and measure concentration of particulate matter (PM), $PM_{2.5}$ and $PM_{10,}$ in µg/m³. Measured concentrations of $PM_{2.5}$ and PM_{10} collected within the BBIC were designated as C_{in} and concentrations of $PM_{2.5}$ and PM_{10} collected outside the BBIC were designated as C_{out}.

The PM_{10} particle size range was chosen to be measured and analysed for this study to simulate coughing, heavy breathing, or sneezing and would generate aerosolised particles ranging from 0.35–10 µm within BBIC chamber during transport of COVID-19 infected patients. These droplets were assumed to be carrying SARS-CoV-2 virus. Larger droplets above 10 µm remained suspended longer in air and might accumulate within the BBIC chamber over time hence increasing the risk of secondary aerosolization. With the same rationale, $PM_{2.5}$ particles were also measured and analysed to assess the effectiveness of BBIC containment and evacuation function. Within the context of this simulation study, we designated the term F_{iso} as a ratio of measured particle concentration within the BBIC (C_{in}) to the measured particle concentration outside of the BBIC (C_{out}), mathematically expressed as: $F_{iso} = C_{in} / C_{out}$.

We designated containment as a state in which an increase in F_{iso} value caused by an increase in C_{in} concentration on a background of relatively low C_{out} concentration

at time 15 minutes, in which the average peak steady state particle concentration was achieved. Evacuation, a state in which a decline in F_{iso} caused by a decrease in both C_{in} and C_{out} concentration during application of negative pressure of from minute 15 to minute 75 (60-minute duration).

The control test, closer ports test,and open ports test were each repeated 3 times. The average data for measured concentration C_{in} and C_{out} was calculated. The F_{iso} for PM_{10} and $PM_{2.5}$ were derived and graphically analysed for each respective test.

OE particle concentration reproducibility test

A qualitative assessment of the OE was carried out using the Vosentech thermal microfogger (Vosentech, Philadephia, PA, USA), a device that generated artificial fog to assess aerosol leak from the OE to the room air. The OE was placed in a fixed designated area without BBIC placed within the enclosure. Each ventilation and access port and the surrounding edges of the OE that were in contact with the floor were sealed and secured to ensure no leak was detected upon initiation of the microfogger machine. Video was recorded with a camera at every side of the OE for a duration of 5 minutes to detect any visible fog leaking from surrounding edges.

After ensuring no fog leak was detected, the AS-LUNG device placed within the OE was switched on, nebulized saline 0.9% was generated within the OE for a duration of 15 minutes and was stopped after 15 minutes, as peak steady state particle concentration was achieved. The AS-LUNG device was left switched on for the next 35 minutes. The concentration of PM_{10} from AS-LUNG data was then collected and graphically analysed. This process was repeated 5 times as a standard measure to obtain the average peak steady state concentration. A graph illustrating a wash-in curve of PM_{10} concentration against time was then plotted (Fig. 1e). Average peak steady state concentration was maintained for 20 minutes.

Control test

In the control test, no BBIC was used within the OE (Fig. 2). The steps outlined in the reproducibility test above were repeated after ensuring all access ports with peripheral edges on all sides of the OE were well sealed. Both AS-LUNG measurement devices were switched on for 60 minutes and the concentration of PM_{10} and $PM_{2.5}$ data were collected.

Closed ports aerosol particle containment and evacuation test

In this test, the BBIC was placed in a designated area within the OE. The steps in the control test were repeated after all the BBIC access ports were tightly zipped (Fig. 2).

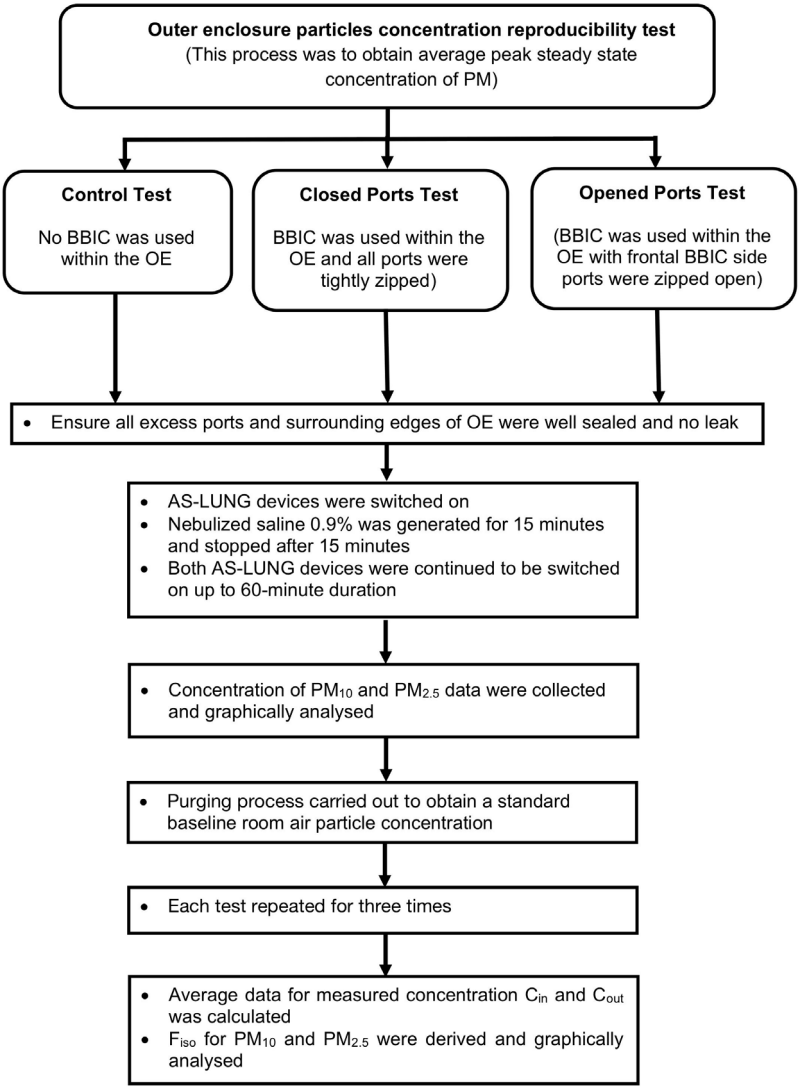

Fig. 2. Flow diagram of the setup for the control test, closed ports test, and open ports test.

Open ports aerosol particle containment and evacuation test

The 4 frontal BBIC side ports were zipped open to simulate the working environment when the healthcare personnel would require access to the patient during transportation. The same steps were repeated (Fig. 2).

Statistical analysis

The PM_{10} and $PM_{2.5}$ concentrations were measured and F_{iso} was calculated and analysed using Apple Numbers version 12.2.1 (7035.0.161) and IBM SPSS statistics version 28.0.0.0 (190). Descriptive statistics were reported. Pearson's correlation coefficient assessed the relationship between PM_{10} and $PM_{2.5}$ F_{iso} over time from minute 15 to minute 75. Repeated measurement ANOVA was used in all 3 tests (control, closed ports, and open ports) to assess significant F_{iso} difference at every time point. Statistical significance was determined to be $p < 0.05$.

Results

Control aerosol particle containment and evacuation test

The control test for both $PM_{2.5}$ and PM_{10} concentrations exhibited relatively constant F_{iso} at each time point from minute 15 to minute 75, respectively (Fig. 3a and 3b). However, F_{iso} was not correlated with time for either PM_{10} readings ($r = 0.47$, $p = 0.282$) nor $PM_{2.5}$ readings ($r = 0.16$, $p = 0.72$). There was a significant difference in F_{iso} between the PM_{10} control test and $PM_{2.5}$ control test at minute 25, 35, 45, 55, and 65, $p < 0.001$, respectively (Fig. 3c). In contrast, differences in concentration of C_{in} and C_{out} for $PM_{2.5}$ were relatively smaller than for PM_{10} which resulted in lower F_{iso} for the $PM_{2.5}$ control test. These findings mean that the position of healthcare workers within the vicinity of the BBIC during static transport would have different exposure rates depending on the dispersion pattern of the generated aerosol.

Aerosol particle containment and evacuation test for PM_{10}

Compared to the control test, F_{iso} PM_{10} in the closed ports test was higher at minute 15 and 25 and declined over time while F_{iso} in the control test remained constant (Fig. 4a). There was a significant difference in F_{iso} between the PM_{10} closed ports test and control test at minute 15 to 75 ($p < 0.05$ respectively). This suggests that the closed ports test contained and evacuated PM_{10} aerosolised particles more effectively than the control test and provided a good physical barrier within the BBIC chamber**.** The F_{iso} of closed ports test was also negatively and strongly correlated with time ($r = -0.79$, $p = 0.035$), which implied effective evacuation of PM_{10} aerosolised particles. As the negative pressure of the BBIC applied from minute 15 for a duration of 60 minutes, C_{in} concentrations within the BBIC decreased over time, hence reduced the F_{iso}.

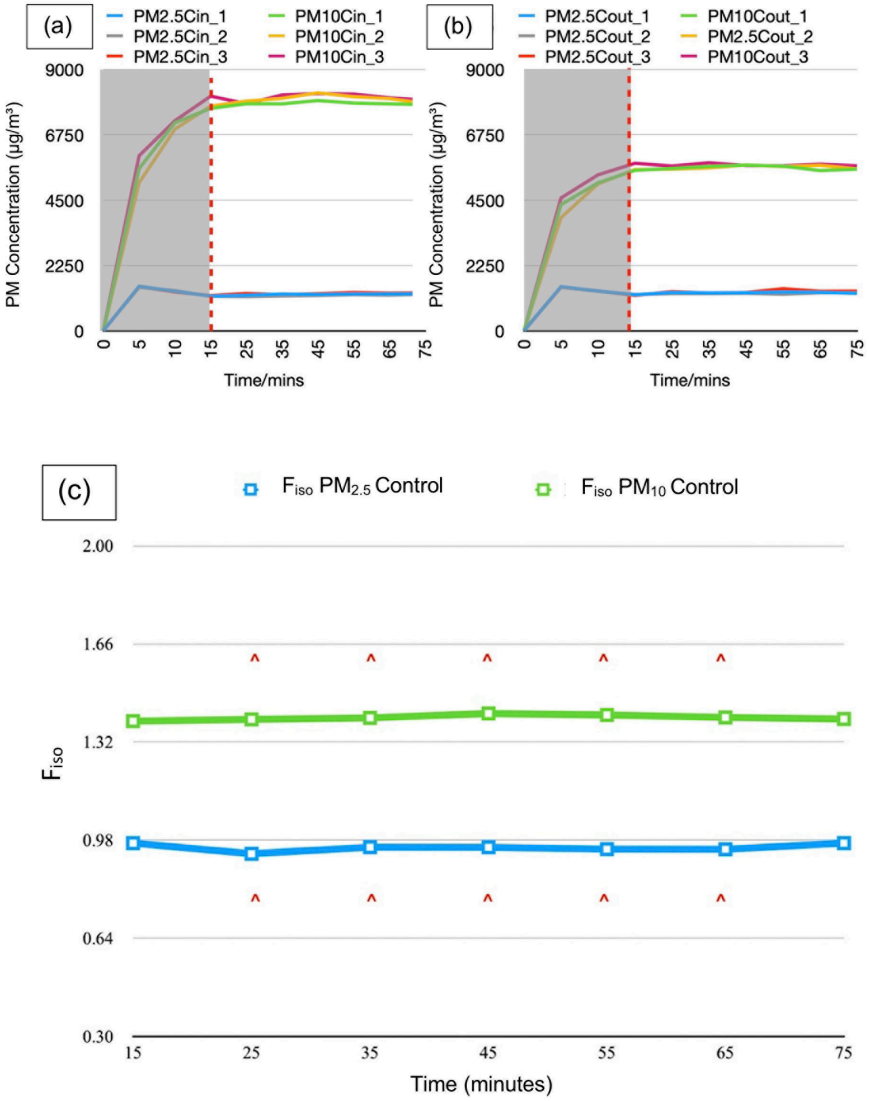

Fig. 3. (a) Concentration (C_{in}) of PM_{10} and $PM_{2.5}$ in control test. *(b)* Concentration (C_{out}) of PM_{10} and $PM_{2.5}$ in control test. *(c)* The F_{iso} of PM_{10} and $PM_{2.5}$ in control test for 60 minutes. Shaded area: duration for generation of nebulized saline within the outer enclosure. (^: $P < 0.05$).

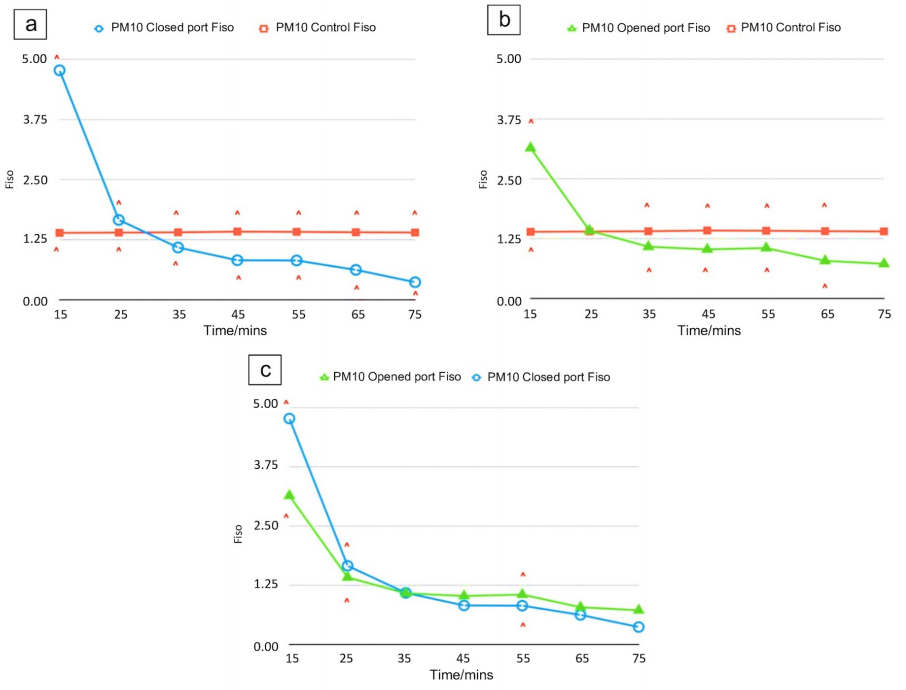

Fig. 4. Comparison of F_{iso} PM_{10}. *(a)* Closed ports test and control test. *(b)* Open ports test and control test. *(c)* Open ports test and closed ports test. (^: $P < 0.05$).

The F_{iso} PM_{10} in the open ports test was higher at minute 15 and then declined overtime while the F_{iso} in the control test remained constant (Fig. 4b). The difference in F_{iso} between PM_{10} in the open ports and control tests was significant at minute 15, 35, 45, 55, and 65 ($p < 0.05$, respectively). The F_{iso} was negatively and strongly correlated with time ($r = -0.79$, $p = 0.035$). These findings suggest that both containment and evacuation of PM_{10} aerosolised particles was more effective in the open ports test compared to the control test. Despite the BBIC's open ports, a barrier was still present to contain generated aerosols.

Both F_{iso} PM_{10} for open ports and closed ports tests declined over minutes 15 to 75. The F_{iso} in the closed ports test was higher at minute 15 and 25 and steadily declined lower than the F_{iso} in the open ports test (Fig. 4c). The difference in F_{iso} between PM_{10} in the open ports and closed ports tests was significant at minute 15, 25, and 55 ($p < 0.001$, 0.036, and 0.029, respectively). These findings imply that the closed ports BBIC was more effective in containing PM_{10} aerosolised particles compared to the open ports BBIC, and that both effectively evacuated PM_{10} aerosolised particles over time. This was due to the closed ports BBIC being

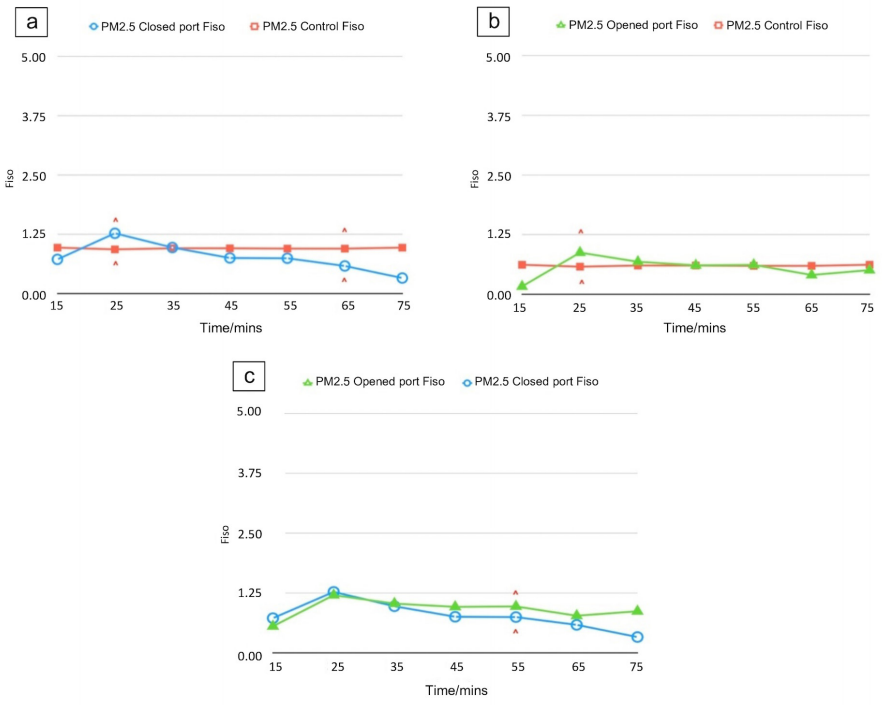

Fig. 5. Comparison of F_{iso} $PM_{2.5}$. *(a)* Closed ports test and control test. *(b)* Open ports test and control test. *(c)* Open ports test and closed ports test. (^: $P < 0.05$).

well sealed, resulting in the BBIC's internal and external environment being well isolated. In the open ports test, the internal chamber of the BBIC communicates with the outer environment of the BBIC within the OE.

Aerosol particle containment and evacuation test for $PM_{2.5}$

Compared to the $PM_{2.5}$ control test, the F_{iso} in the $PM_{2.5}$ closed ports test was higher at minute 25 and then declined over time, while the F_{iso} in the control test remained constant (Fig. 5a). The correlation between F_{iso} in the $PM_{2.5}$ closed ports test with time was not significant (r = -0.72, p = 0.066). The difference in F_{iso} between the closed ports test and control test was significant at minute 25 and 65 (p = 0.003 and 0.003, respectively). From this data we deduce that there was insufficient evidence to suggest that the closed ports and control tests would effectively contain and evacuate $PM_{2.5}$ aerosolised particles.

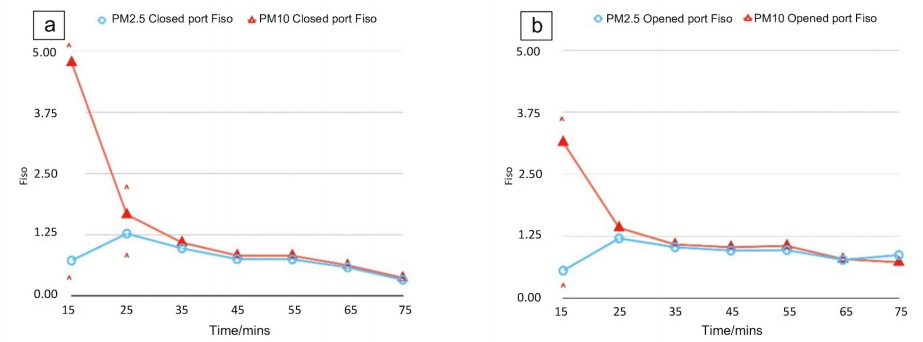

Fig. 6. (a) Comparison of F_{iso} (PM_{10}) and F_{iso} ($PM_{2.5}$) in closed ports test. *(b)* Comparison of F_{iso} (PM_{10}) and F_{iso} ($PM_{2.5}$) in open ports test. (^: $P < 0.05$).

Compared to the $PM_{2.5}$ control test, the F_{iso} in the open ports test was lower at minute 15, and then again at minute 65 to 75 (Fig. 5b) while the F_{iso} in the control test remained constant. The correlation between the F_{iso} for $PM_{2.5}$ in the open ports test and time was poor ($r = 0.015$, $p = 0.975$). The difference in F_{iso} was significant at minute 25 ($p = 0.017$). In general, these findings imply that both the control test and open ports test did not effectively contain and evacuate $PM_{2.5}$ aerosolised particles.

The F_{iso} for $PM_{2.5}$ in the closed ports test increased at minute 25 and decreased at minute 35 to 75 (Fig. 5c). The F_{iso} difference was significant at minute 55 ($p = 0.036$). The F_{iso} for $PM_{2.5}$ in both the closed and open ports tests were poorly correlated with time ($r = -0.72$, $p = 0.066$ and $r = 0.015$, $p = 0.975$, respectively). From this data, we deduce that there was insufficient evidence to suggest that the closed ports test and open ports test were more effective in containing and evacuating $PM_{2.5}$ aerosolised particles.

Comparison between aerosol particle containment and evacuation test for PM_{10} and $PM_{2.5}$

The F_{iso} for both PM_{10} and $PM_{2.5}$ in the closed ports tests decreased from minute 15 to 75. However, the F_{iso} for PM_{10} in the closed ports test was higher at minute 15 and 25 (Fig. 6a). The difference in F_{iso} for PM_{10} compared to that of $PM_{2.5}$ readings was significant at minute 15 and 25 ($p < 0.001$, respectively). This suggests that closed ports BBIC was more effective in containing PM_{10} compared to $PM_{2.5}$ aerosolised particles.

Compared to $PM_{2.5}$ open ports, the F_{iso} for PM_{10} open ports decreased over time from minute 15 to 75 while F_{iso} for $PM_{2.5}$ in the open ports test increased from

minute 15 to 25, followed by a minimal decline from minute 25 to 75 (Fig. 6b). The F_{iso} for PM_{10} in the open ports test was higher than that of the $PM_{2.5}$ open ports test at minute 15 and 25. The difference in F_{iso} of PM_{10} compared to that of $PM_{2.5}$ was significant at minute15 ($p < 0.001$). This suggests that the open ports BBIC was more effective in containing PM_{10} compared to $PM_{2.5}$ aerosolised particles.

Discussion

This simulation study was designed to test the effectiveness of BBIC in containing and evacuating aerosolised particles. Using F_{iso} as a ratio of aerosolised particle concentration within the BBIC (C_{in}) to the aerosolised particle concentration outside the BBIC (C_{out}), we were able to estimate trends that signify effective containment and evacuation function of the BBIC during static transport of COVID-19 patients.

Aerosol exposure is clinically relevant because both aerosol and droplets constitute an exposure risk for COVID-19. [34,35] Our simulations demonstrated, in general, that a well-utilized, functioning BBIC with closed ports and application of negative pressure was able to effectively contain and evacuate PM_{10} aerosolised particles. In real clinical scenarios, the utility of BBIC with all the ports closed would reduce PM_{10} aerosol concentration carrying SARS-CoV-2 in the surrounding environment and therefore reduce the risk of aerosol exposure to healthcare workers in the vicinity of the BBIC. The BBIC contains the spread and evacuates the infective aerosols via application of negative pressure, which directs the generated aerosols towards the HEPA filters. This can be beneficial for different situations as the utility of isolation chambers has been shown to reduce medical cessation in emergency departments and reduce delays attributed to disinfection of computed tomography machines in radiology departments.[25]

Conversely, the control group represents healthcare workers transporting COVID-19 patients without using a BBIC. As a result, C_{out} concentrations in this scenario would be higher than that of clinical scenarios where the BBIC is utilized. Higher C_{out} levels mean that the generated aerosol concentration in environment is increased, therefore increasing the risk of exposure of aerosol carrying SARS-CoV-2 to healthcare workers in the vicinity of the BBIC.

In contrast, opening the access ports during static transport of COVID-19 patients would cause an increase in PM_{10} particle concentration in the environment, hence increasing the risk of droplet exposure to healthcare workers in the vicinity of the BBIC. Nonetheless, the utility of the BBIC itself, irrespec-

tive of access ports being open or closed, results in less PM_{10} particle concentrations in the environment air and therefore reduces the risk of droplet exposure to healthcare workers during transport. The effect of applying negative pressure is analysed in other quantitative studies involving isolation hood and intubation box models, which have shown reductions in generated particulate count during application of negative pressure, while isolation without negative pressure shows retention of particulate count within the chamber.[22,29] The importance of applying negative pressure during BBIC usage should be emphasized because retention of aerosolised particles may contribute to secondary aerosolization.[28,31]

Interestingly, when comparing the $PM_{2.5}$ simulations in our study, there was insufficient evidence to suggest that control, closed ports, and open ports tests were more effective in containing and evacuating $PM_{2.5}$ aerosolised particles. This could be attributed to the possibility of BBIC equipment leak to smaller diameter aerosolised particles or the intrinsic characteristics of $PM_{2.5}$ aerosolised particles, such as size, composition, and density, playing a role in aerosol movement direction.[20-22] Small droplets have been shown to freely travel in the air and carry their viral content meters and tens of meters from where they originated.[36] In real clinical scenarios, this would mean that the environment air would have higher $PM_{2.5}$ particle concentration carrying SARS-CoV2, which increases the risk of droplet exposure to healthcare workers in the vicinity of the BBIC during static transport, irrespective of whether the access ports are opened or closed.

Furthermore, we noted F_{iso} differences between PM_{10} and $PM_{2.5}$ when measuring generated aerosolised particles in separate positions of AS-LUNG sensors. In real clinical scenarios, these findings suggest that the position of healthcare workers within the vicinity of the BBIC during static transport of COVID-19 patients entails different exposure rates depending on the dispersion pattern of generated aerosols.[28,37] These differences would also require further mathematical computational fluid dynamics simulations to predict the pattern of dispersion of generated aerosol and as such, should be the subject of future discussion not relevant to this current study.

This simulation study was carried out to quantitatively assess the effectiveness of containing and evacuating aerosolised particles in an isolation chamber of a specific brand. Comparisons of isolation chambers of various designs are required. The simulation was designed to assess quantitative data during static transport and not dynamic transport of patients. We did not consider simulations involving variable patient conditions including coughing, sneezing, or heavily breathing. The nature of this study is simulation-only, where patient-derived aerosols may differ in behaviour from nebulized saline.

We recommend proper usage of the BBIC, ensuring the equipment is well charged before transport, regular maintenance of the negative pressure function and the HEPA filters, regular disinfection of the internal chambers, as well as proper education and training of healthcare workers to ensure safety during BBIC usage. We suggest computational fluid dynamics simulation software to be considered in future studies to assess the variability of aerosol movement and dispersion.

Conclusion

The closed and open BBIC ports effectively contained and evacuated PM_{10} aerosolised particles during simulation of static transport of COVID-19 patients. The BBIC contained and evacuated PM_{10} more effectively than $PM_{2.5}$ aerosolised particles.

Declarations

Ethics approval and informed consent
This simulation study was conducted within the two-week duration in August 2022 at the Department of Anaesthesiology and Intensive Care, Hospital Canselor Tuanku Muhriz following the approval from Secretariat of Research and Innovation, Faculty of Medicine, Universiti Kebangsaan Malaysia and institutional Research and Ethics Committee (Code: JEP-2022-212).

Competing interests
Dr. Azarinah Izaham and Dr. Rufinah Teo serve in Malaysian Journal of Anaesthesiology's Editorial Board. Neither were involved in the publication process prior to acceptance. Malaysian Journal of Anaesthesiology employs a double-blind review system. The remaining authors have no competing interests to disclose.

Funding
None to declare.

Acknowledgements
None to declare.

References

1. Li Q, Guan X, Wu P, et al. Early Transmission Dynamics in Wuhan, China, of Novel Coronavirus-Infected Pneumonia. N Engl J Med. 2020;382(13):1199-1207. https://doi.org/10.1056/nejmoa2001316
2. Tran K, Cimon K, Severn M, Pessoa-Silva CL, Conly J. Aerosol generating procedures and risk of transmission of acute respiratory infections to healthcare workers: a systematic review. PLoS One. 2012;7(4):e35797. https://doi.org/10.1371/journal.pone.0035797
3. Gómez-Ochoa SA, Franco OH, Rojas LZ, et al. COVID-19 in Health-Care Workers: A Living Systematic Review and Meta-Analysis of Prevalence, Risk Factors, Clinical Characteristics, and Outcomes [published correction appears in Am J Epidemiol. 2021 Jan 4;190(1):187]. Am J Epidemiol. 2021;190(1):161-175. https://doi.org/10.1093/aje/kwaa191
4. Kursumovic E, Lennane S, Cook TM. Deaths in healthcare workers due to COVID-19: the need for robust data and analysis. Anaesthesia. 2020;75(8):989-992. https://doi.org/10.1111/anae.15116
5. Astuti I, Ysrafil. Severe Acute Respiratory Syndrome Coronavirus 2 (SARS-CoV-2): An overview of viral structure and host response. Diabetes Metab Syndr. 2020;14(4):407-412. https://doi.org/10.1016/j.dsx.2020.04.020
6. Duguid JP. The size and the duration of air-carriage of respiratory droplets and droplet-nuclei.J Hyg (Lond). 1946;44(6):471-479. https://doi.org/10.1017/s0022172400019288
7. Atkinson J, Chartier Y, Pessoa-Silva CL, et al., editors. Natural Ventilation for Infection Control in Health-Care Settings. Geneva: World Health Organization; 2009.
8. Bourouiba L. Turbulent Gas Clouds and Respiratory Pathogen Emissions: Potential Implications for Reducing Transmission of COVID -19. JAMA. 2020;323(18):1837–1838. https://doi.org/10.1001/jama.2020.4756
9. Morawska L, Cao J. Airborne transmission of SARS-CoV-2: The world should face the reality. Environ Int. 2020;139:105730. https://doi.org/10.1016/j.envint.2020.105730
10. Booth TF, Kournikakis B, Bastien N, et al. Detection of Airborne Severe Acute Respiratory Syndrome (SARS) Coronavirus and Environmental Contamination in SARS Outbreak Units. The JID. 2025;191:1472–1477. https://doi.org/10.1086/429634
11. Liu Y, Ning Z, Chen Y, et al. Aerodynamic analysis of SARS-CoV-2 in two Wuhan hospitals. Nature 582, 557–560 (2020). https://doi.org/10.1038/s41586-020-2271-3
12. Guo ZD, Wang ZY, Zhang SF, et al. Aerosol and Surface Distribution of Severe Acute Respiratory Syndrome Coronavirus 2 in Hospital Wards, Wuhan, China, 2020. Emerg Infect Dis. 2020;26(7):1583-1591. https://doi.org/10.3201/eid2607.200885
13. Birgand G, Peiffer-Smadja N, Fournier S, Kerneis S, Lescure F, Lucet J. Assessment of Air Contamination by SARS-CoV-2 in Hospital Settings. JAMA Netw Open. 2020;3(12):e2033232. https://doi.org/10.1001/jamanetworkopen.2020.33232
14. Lindsley WG, Pearce TA, Hudnall JB, et al. Quantity and size distribution of cough-generated aerosol particles produced by influenza patients during and after illness. J Occup Environ Hyg. 2012;9(7):443-449. https://doi.org/10.1080/15459624.2012.684582
15. World Health Organization. Modes of transmission of virus causing COVID-19: implications for IPC precaution recommendations. Sci Brief (2020).

16. Lindsley WG, Noti JD, Blachere FM, et al. Viable Influenza A Virus in Airborne Particles from Human Coughs, Journal of Occupational and Environmental Hygiene. 2025;12(2):107-113. https://doi.org/10.1080/15459624.2014.973113
17. Lee J, Yoo D, Ryu S, et al. Quantity, size distribution, and characteristics of cough-generated aerosol produced by patients with an upper respiratory tract infection. Aerosol Air Qual. Res. 2019;19:840-853. https://doi.org/10.4209/aaqr.2018.01.0031
18. Morawska L. Droplet fate in indoor environments, or can we prevent the spread of infection? Indoor Air. 2006;16(5):335-347. https://doi.org/10.37934/cfdl.17.2.115135
19. Xie X, Li Y, Chwang A, Ho P, Seto W. How far droplets can move in indoor environments? revisiting the Wells evaporation falling curve. Indoor Air. 2007;17(3):211-225. https://doi.org/10.1111/j.1600-0668.2007.00469.x
20. Gralton J, Tovey E, McLaws ML, Rawlinson WD. The role of particle size in aerosolised pathogen transmission: a review. J Infect. 2011;62(1):1-13. http://dx.doi.org/10.1016/j.jinf.2010.11.010
21. Wei J, Li Y. Airborne spread of infectious agents in the indoor environment. Am J Infect Control. 2016;44(9 Suppl):S102-S108. https://doi.org/10.1016/j.ajic.2016.06.003
22. Le HD, Novak GA, Janek KC, et al. A novel box for aerosol and droplet guarding and evacuation in respiratory infection (BADGER) for COVID-19 and future outbreaks. Sci Rep. 11, 3179 (2021). https://doi.org/10.1038/s41598-021-82675-6
23. www.biobase.cc/Biological-Isolation-Chamber-pd46826995.html
24. Tsai SH, Tsang CM, Wu HR, et al. Transporting patient with suspected SARS. Emerg Infect Dis. 2004;10(7):1325-1326. https://doi.org/10.3201/eid1007.030608
25. Kim SC, Kong SY, Park GJ, et al. Effectiveness of negative pressure isolation stretcher and rooms for SARS-CoV-2 nosocomial infection control and maintenance of South Korean emergency department capacity. Am J Emerg Med. 2021;45:483-489. https://doi.org/10.1016/j.ajem.2020.09.081
26. Dindart JM, Peyrouset O, Palich R, et al. Aerial medical evacuation of health workers with suspected Ebola virus disease in Guinea Conakry-interest of a negative pressure isolation pod-a case series. BMC Emerg Med. 17, 9 (2016). https://doi.org/10.1186/s12873-017-0121-x
27. Begley JL, Lavery KE, Nickson CP, Brewster DJ. The aerosol box for intubation in coronavirus disease 2019 patients: an in-situ simulation crossover study. Anaesthesia. 2020;75(8):1014-1021. https://doi.org/10.1111/anae.15115
28. Fidler RL, Niedek CR, Teng JJ, et al. Aerosol Retention Characteristics of Barrier Devices. Anesthesiology. 2021;134(1):61-71. https://doi.org/10.1097/aln.0000000000003597
29. Lang AL, Shaw KM, Lozano R, Wang J. Effectiveness of a negative-pressure patient isolation hood shown using particle count. Br J Anaesth. 2020 Sep;125(3):e295-e296. https://doi.org/10.1016/j.bja.2020.05.002
30. Owen MK, Ensor DS, Sparks LE. Airborne particle sizes and sources found in indoor air. Atmos Environ Gen Top. 1992;26:2149–2162.
31. Cubillos J, Querney J, Rankin A, Moore J, Armstrong K. A multipurpose portable negative air flow isolation chamber for aerosol-generating procedures during the COVID-19 pandemic. Br J Anaesth. 2020 Jul;125(1):e179-e181 https://doi.org/10.1016/j.bja.2020.04.059

32. Ramdan MI, Abd Rahim I, Nik Ab Rahman NH, et al. Development Of an Affordable Negative-Pressure Full-Body Isolation Pod for Covid-19 Patient Transportation. Journal of Advanced Research in Fluid Mechanics and Thermal Sciences. 2021;88(3):137-144. https://doi.org/10.37934/arfmts.88.3.137144
33. Blood TC Jr, Perkins JN, Wistermayer PR, et al. COVID-19 Airway Management Isolation Chamber. Otolaryngol Head Neck Surg. 2021 Jan;164(1):74-81. https://doi.org/10.1177/0194599820942500
34. Lu J, Gu J, Li K, Xu C, Su W, Lai Z, Zhou D, Yu C, Xu B, Yang Z. COVID-19 outbreak associated with air conditioning in restaurant, Guangzhou, China, 2020. Emerg Infect Dis. 2020; 26: 1628–31. https://doi.org/10.3201/eid2607.200764
35. National Academies of Sciences, Engineering, and Medicine. Rapid Expert Consultation on the Possibility of Bioaerosol Spread of SARS–CoV-2 for the COVID-19 Pandemic (April 1, 2020). 2020, Washington, DC: National Academies Press.
36. Morawska L, Johnson GR, Ristovski ZD, et al. Size distribution and sites of origin of droplets expelled from the human respiratory tract during expiratory activities. Journal of Aerosol Science. 2009;40(3):256-269. https://doi.org/10.1016/j.jaerosci.2008.11.002.
37. Li Y, Huang X, Yu IT, Wong TW, Qian H. Role of air distribution in SARS transmission during the largest nosocomial outbreak in Hong Kong. Indoor Air. 2005 Apr;15(2):83-95. https://doi.org/10.1111/j.1600-0668.2004.00317.x